Beams-doc-1598-v1
March 9, 2005

Cancellation of the Proton Contamination on the TeV BPM Anti-proton Channels

Rob Kutschke, CD/EXP

Abstract

This note looks at some new ideas about the cancellation of the proton contamination on the anti-proton channels of the upgraded Tevatron BPM electronics. The note also presents data on how the parameters of the cancellation vary from BPM to BPM and how they vary with time. Part of this new parameterization is the use of a complex valued position variable. Some properties of this new position variable are also shown. This note is a status report of a work in progress.

1 Introduction: A New Parameterization

In previous work, the cancellation of the proton contamination on the anti-proton channels was done using the equations,

$$\begin{aligned} A'_{\bar{p}} &= A_{\bar{p}} - aA_p - bB_p \\ B'_{\bar{p}} &= B_{\bar{p}} - cB_p - dA_p \end{aligned} \quad (1)$$

where A and B are the raw complex numbers (I, Q) from the Echotek, where the primed quantities are the estimate of the true anti-proton signal, after removal of the proton contamination, and where the constants a, b, c, d are determined empirically. The method used to determined the constants is described as model 1 in Beams-doc-988. Also in previous work, the proton position was defined as the real number,

$$P = 26\frac{|A_p| - |B_p|}{|A_p| + |B_p|} \quad (2)$$

In the work presented here, a new parameterization, will be used. First, the position is defined as the complex number,

$$P = 26\frac{A_p - B_p}{A_p + B_p}. \quad (3)$$

With this definition, the cancellation equations can be written as,

$$\begin{aligned} A'_{\bar{p}} &= A_{\bar{p}} - a_0(A_p + B_p)\left[1 - a_1 P\right] \\ B'_{\bar{p}} &= B_{\bar{p}} - b_0(A_p + B_p)\left[1 - b_1 P\right], \end{aligned}$$

where A and B are defined as before, and where the constants a_0, a_1, b_0, b_1 are determined empirically. A little algebra will show that one can express a, b, c, d in terms of a_0, a_1, b_0, b_1 and that these equations are really the same as the Equation 1. In the following I will sometimes refer to a_0 and b_0 as the intensity coefficients and to a_1 and b_1 as the position coefficients.

The reason for introducing this new parameterization is that the parameters have a simpler physical interpretation. For example the coefficients a_0 and b_0 are related to the mis-directionality of the pickups. Also, one expects that a_1 and b_1 will have opposite phases. This parameterization also has a natural extension, to include the beam position in the unmeasured transverse coordinate, $P_\perp$,

$$\begin{aligned} A'_{\bar{p}} &= A_{\bar{p}} - a_0(A_p + B_p)\,[1 - a_1 P - a_2 P_\perp] \\ B'_{\bar{p}} &= B_{\bar{p}} - b_0(A_p + B_p)\,[1 - b_1 P - b_2 P_\perp]\,, \end{aligned}$$

To make this extension work, it will have to written in terms of a real $P_\perp$, because meaningful phase information on $P_\perp$ is not likely to be available.

2 The Complex Position

One complication introduced by the complex position is that one cannot make a fast time plot of a complex quantity. There are two simple ways to make a real quantity from this complex quantity, $\Re(P)$ or $|P|$. The choice of $\Re(P)$ is equivalent to taking the component of the numerator which is in phase with the denominator,[1] the technique which has been suggested for removing the head-tail effect noted by Valeri Lebedev. I am not sure of the physical meaning of the absolute value. The following plots show some properties of these new definitions.

The top plot in Figure 1 shows the traditional position (Equation 2) plotted against time during the first hour of a shot. The horizontal axis is time, measured in units of 1 second, from the start of the data sample. All plots on this page cover the same time interval. One can see a stable position of about -1 mm during proton injection, the opening of the helix, a stable position of about -4.5 mm during anti-proton injection, beam motion during the ramp, squeeze and initiation of collisions and, finally a stable position during HEP collisions.

The second plot in Figure 1 shows the difference ($\arg(B_p) - \arg(A_p)$), plotted vs time. This phase difference is very stable during proton injection and drifts only a small amount during anti-proton injection. It also changes only a small amount during the substantial beam motion as the beams are ramped and brought into collision. This suggests a possible variation of the model, to use $\Re(P)$ or $|P|$ instead of P in equation 3. If this works, it will smooth the way to including the $P_\perp$ correction.

[1] To show this, multiply the numerator and denominator on the RHS of equation 3 by $(A_p + B_p)^*$.

The third plot shows the difference $(\Re(P_{\mathrm{complex}}) - P_{\mathrm{traditional}})$ plotted vs time. This plot has a lot of structure but the scale of the structure is very small, about 20 μm full scale. The conclusion is that this definition of the position is very close to the traditional definition of position.

The bottom plot shows $\Im(P_{\mathrm{complex}})$. The imaginary part is quite significant, about 1.5 mm, but its variations across the shot are of intermediate size, about 100 μm. One possible interpretation of this plot is that a non-zero $\Im(P_{\mathrm{complex}})$ can be generated by the head-tail effect suggested by Valeri Lebedev; but that is far from being established as the source of this imaginary part.

The top plot in Figure 2 is a repeat of the top plot on the previous page. The bottom plot shows $|P_{\mathrm{complex}}| - P_{\mathrm{traditional}}$ vs time. This definition of position is quite different than the traditional definition. I don't yet understand what this means.

3 Cancellation of the Proton Contamination

The next plots show how the parameters of the proton cancellation differ from BPM to BPM and how they change with time. These data are derived from 7 shots measured in the A3 and B3 houses and from 5 shots measured in the C3 house; this study started before the new electronics were installed in the C3 house. For each shot, the IQ values for all channels were extracted from the lumberjack data logger, covering the time from the start of the shot to the start of HEP running. For each shot the time at which the helix opened was identified and data from just before and just after the helix opening were used to compute the cancellation parameters. This calibration technique is described as model 1 in Beams-doc-988; only the algebra of the parameterization has changed.

The top plot in Figure 3 shows the values of a_0 determined by this method for all 24 BPMs in the A3, B3 and C3 houses. For each BPM in A3 and B3 there are 7 circles plotted, one for each of the 7 shots. For each BPM in C3 there are 5 circles plotted. In most cases the circles fall almost on top of each other but in a few cases, HA38, VB33 and HB36, the positions of the circles vary a lot. At these BPMs the helix opens almost 100% in the unmeasured direction. So the algorithm to compute the cancellation parameters has only a small lever arm, thereby giving unstable results. A different algorithm needs to be developed for this BPMs and they will be suppressed in the following work.

The bottom plot in Figure 3 shows the same data as the upper plot, but with the noisy channels suppressed and with an expanded scale. The horizontal channels are drawn in blue and the vertical channels are drawn in green. On this scale it can be seen that, for many channels, the calibration does vary a little from shot to shot. There is no obvious structure in either the horizontal or vertical BPMs.

A later version of this note will show that even channels which have no discernible shot to shot variation on this plot, do have significant changes in calibration from shot to shot. So this plot is only useful for crude studies of the stability of these calibration constants.

The four plots in Figure 4 show, for each BPM and for the 5 or 7 shots, the magnitudes and phases of the parameters a_0 and b_0. Again the blue points are for horizontal BPMS and the green points are for the vertical BPMs. Most BPMs show a small, but discernible, variation from shot to shot. A few BPMs have no discernible variation. The only quantity with a large variation is the phase of b_0 for BPM 16 (VB39), highlighted in red. Inspection of the $|b_0|$ plot shows that this BPM, highlighted in red, has a very small magnitude for b_0; therefore its phase is poorly defined.

One thing to notice in this plot is the mean values of $|a_0|$ and $|b_0|$, both about 0.07. The attenuations of the filter board attenuators on the proton channels are about 3 times higher attenuation than those on the anti-proton channels. So one can estimate the typical mis-directionality of the pickups as as about $0.07/3 = 0.02$.

The four parts of Figure 5 show the magnitude and phase of a_1 and b_1. Again there are a few quantities, highlighted in red, which have a large spread in their values; in all of these cases, the corresponding value of a_0 or b_0 is small. So these are understood.

There are two main features in these plots. The values of $|a_0|$ and $|b_0|$ are both clustered around 0.1 mm^{-1}; that is, all of the plates have position coefficients of similar magnitude. Because beam motions of 5 to 10 mm are not uncommon, the position coefficient is actually quite large. The second feature is that the values of $\arg(a_1)$ cluster around $\pm\pi$, while those of $\arg(b_1)$ cluster near zero. This confirms the expectation that the position coefficients should have opposite phase.

4 Summary and Conclusions

These studies show that the cancellation coefficients vary a great deal from one BPM to the next. This variation is much larger than the variation among several shots for one BPM. So, as expected, it will be necessary to maintain cancellation constants separately for each BPM.

In this new parameterization, the parameters $|a_0|$, $|b_0|$ and the phase difference, $\arg(b_1) - \arg(a_1)$, make physical sense. The magnitudes of the position coefficents, $|a_1|$ and $|b - 1|$ are quite large.

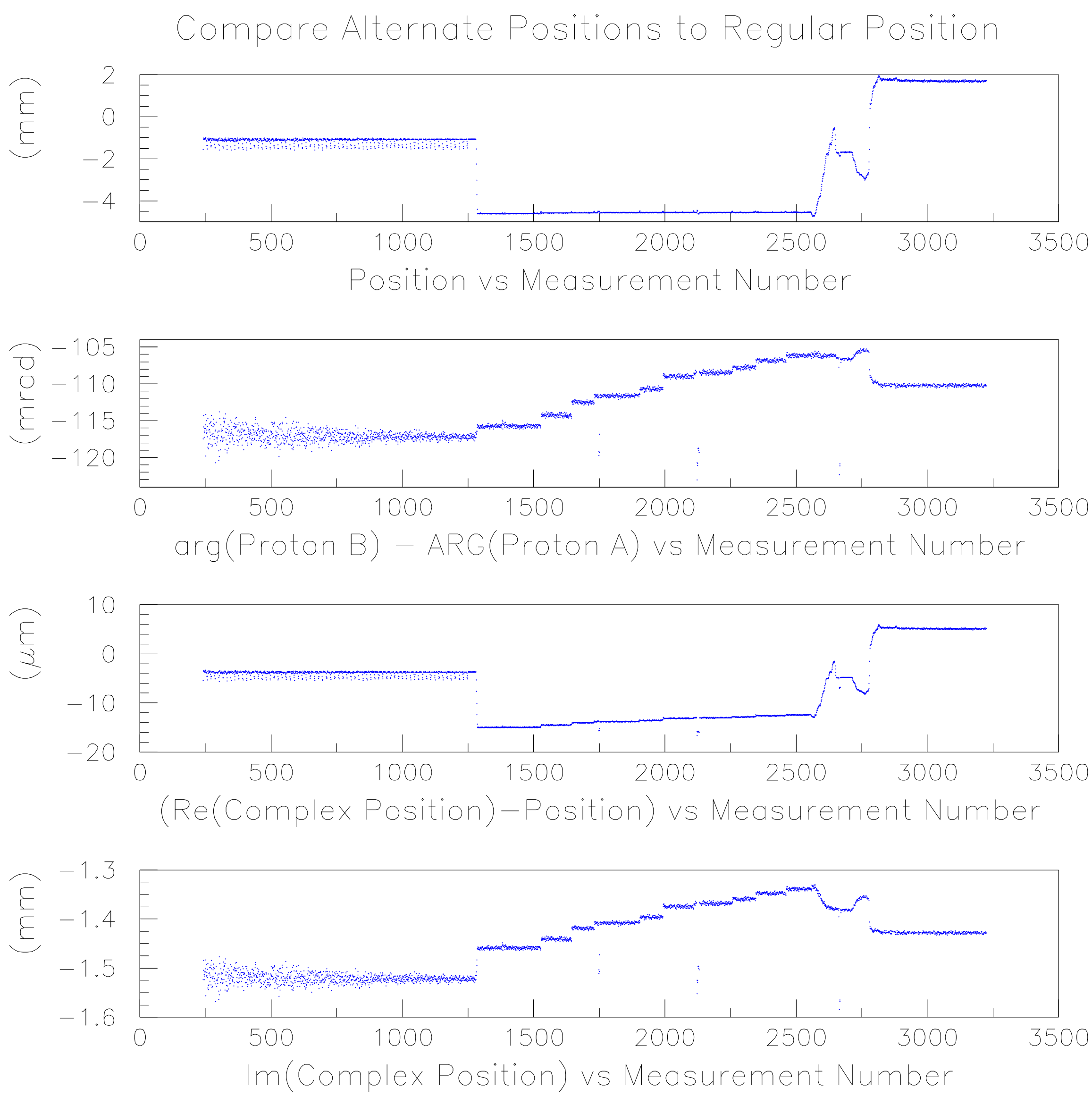

Figure 1: Comparison of the complex position (Equation 3) with the traditional position (Equation 2). See the text for details.

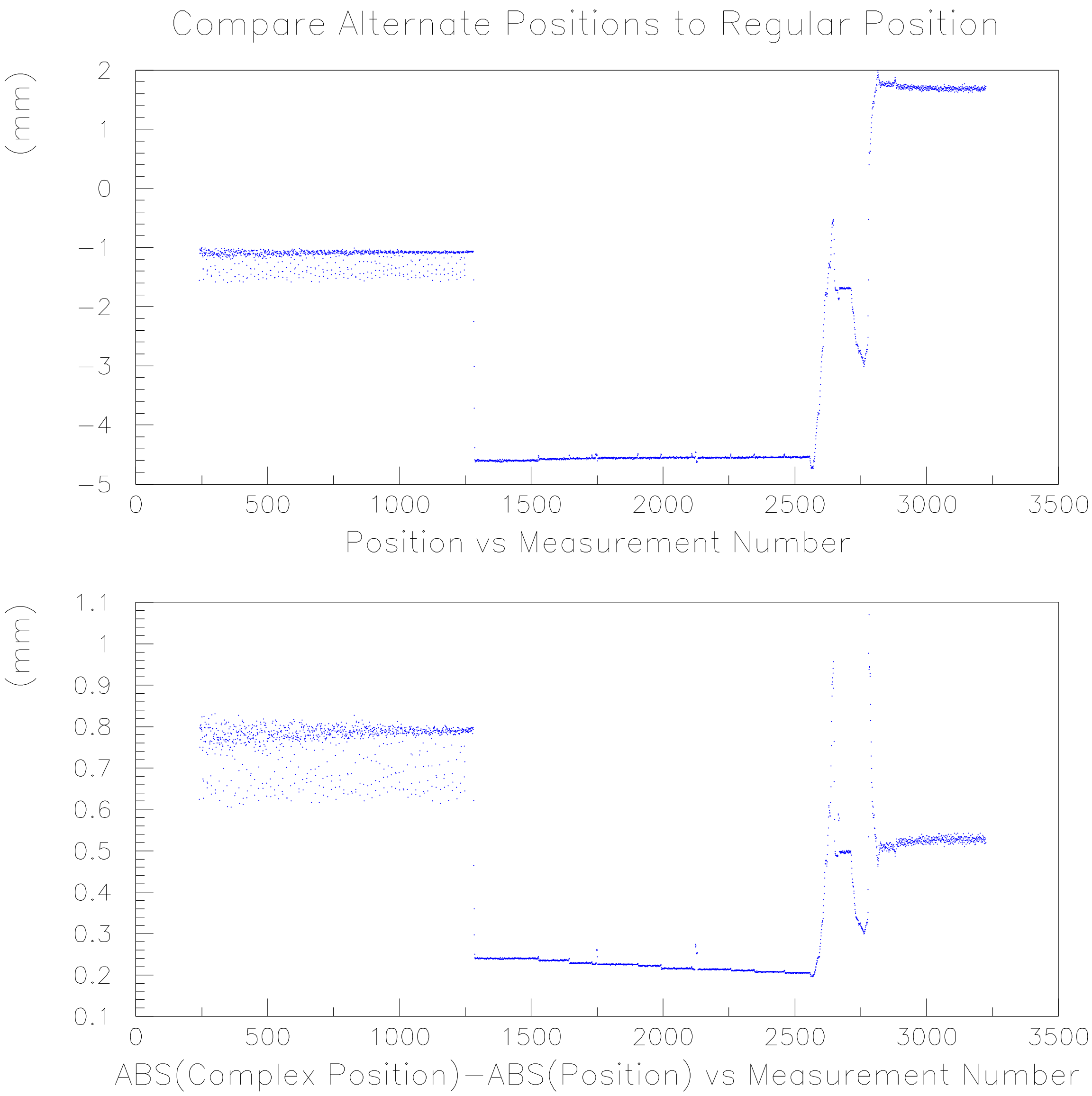

Figure 2: Comparison of the complex position (Equation 3) with the traditional position (Equation 2). See the text for details.

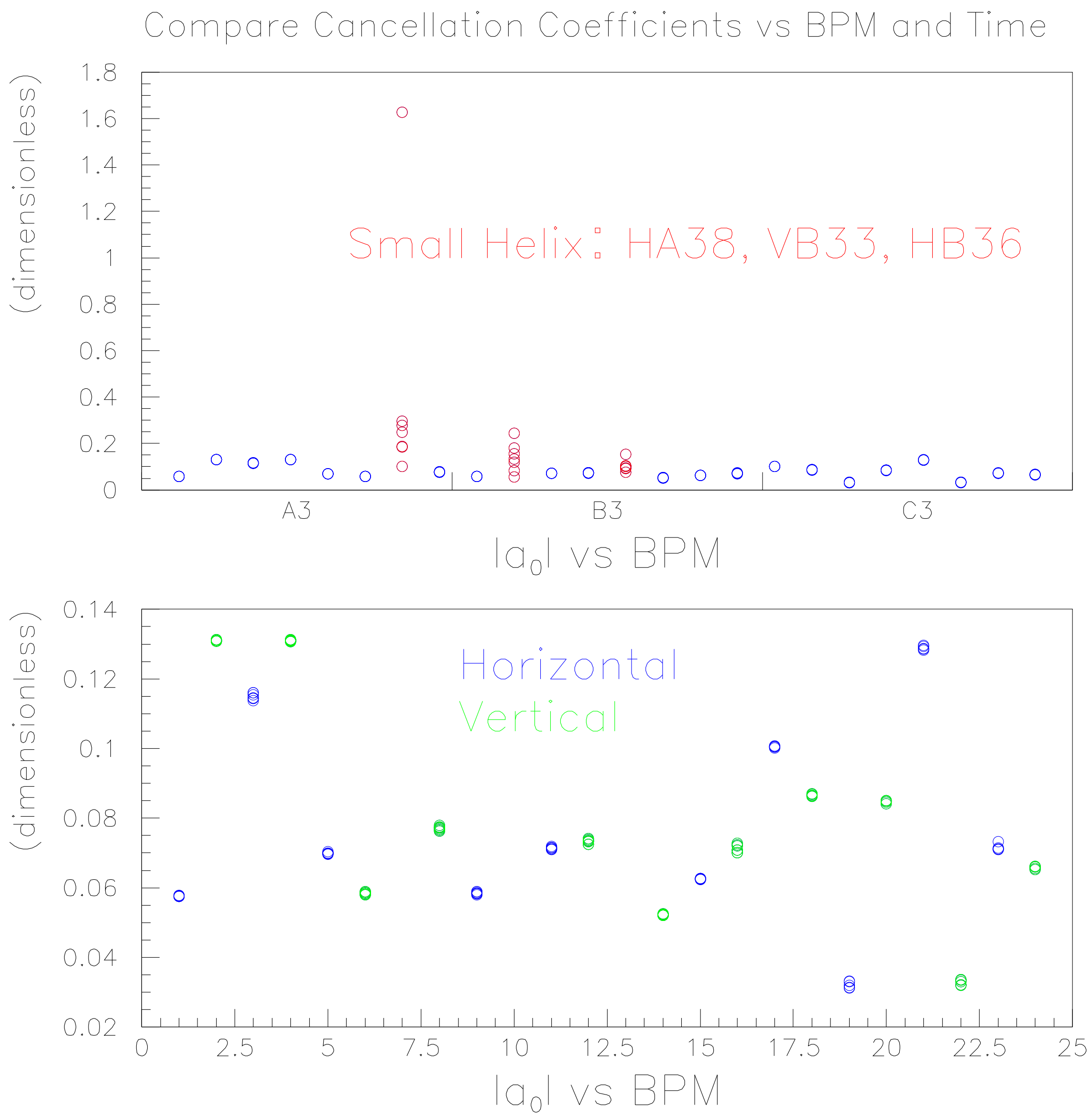

Figure 3: Study of how $|a_0|$ varies from BPM to BPM and how it varies with time. In each column there are 7 circles for the BPMS in the A3 and B3 houses and 5 circles for the BPMs in the C3 house. But many circles lie on top of each other. Additional discussion can be found in the text.

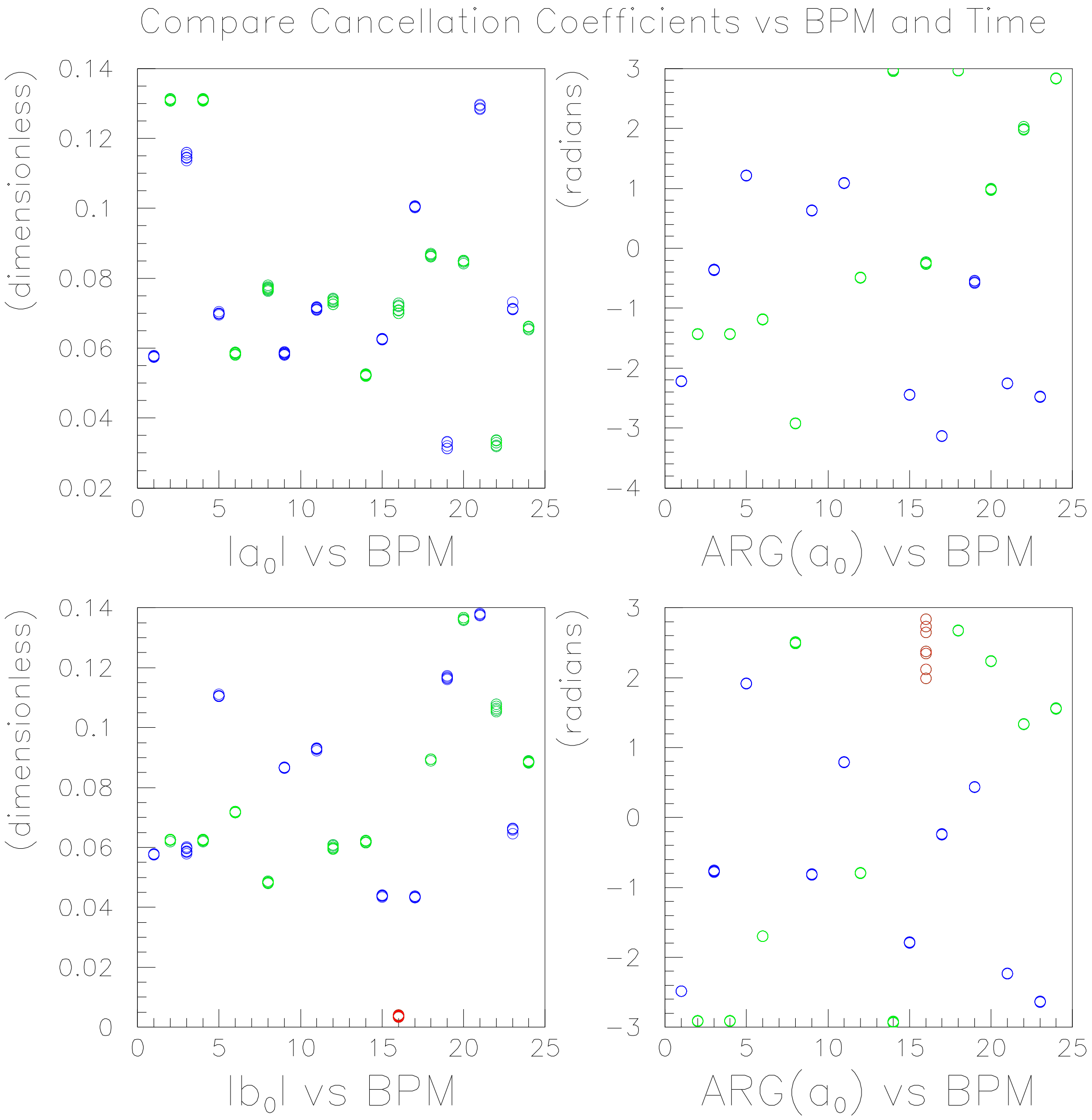

Figure 4: Study of how the magnitude and phase of the intensity coefficients vary from BPM to BPM and how they vary with time. Details can be found in the text.

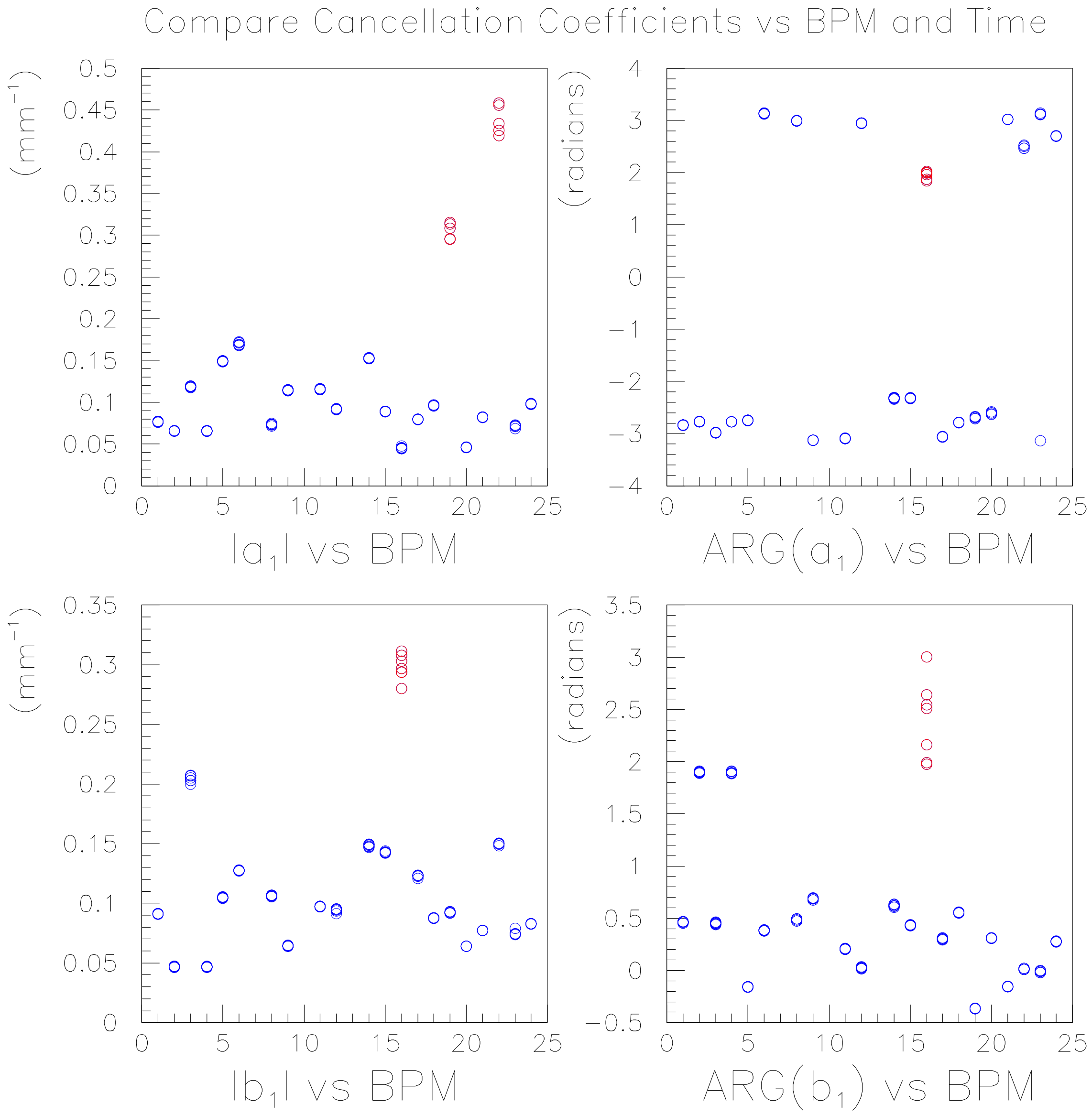

Figure 5: Study of how the magnitude and phase of the position coefficients vary from BPM to BPM and how they vary with time. Details can be found in the text.